

## Core-electron excitation edges in metallic Ni, Cu, Pt, and Au

R. E. Dietz and E. G. McRae

*Bell Laboratories, Murray Hill, New Jersey 07974*

J. H. Weaver

*Synchrotron Radiation Center, University of Wisconsin-Madison, Stoughton, Wisconsin 53589*

(Received 29 June 1979)

The shapes of core excitation edges with  $E_B < 150$  eV are reported for Ni, Cu, Pt, and Au. The spectra are interpreted as arising from the interference of excitations of core electrons into conduction-band states of  $d$  symmetry with excitations of  $d$  electrons into continuum states of  $f$  symmetry well above the vacuum level. In all cases excitation of core electrons into  $d$  conduction-band states hybridized into the  $sp$  conduction bands is important, but in the metals Ni and Pt, which have partially filled  $d$  bands, the excitation of core electrons into unhybridized  $d$  states outweighs the contributions of the hybridized  $d$  states at the Fermi edge. The line shapes due to the spectral densities resulting from excitations into the unhybridized part are accurately described by Fano interferences due to configuration interaction between a spin-orbit component of a core-hole state and the  $d$ -electron continua of partial waves indexed by the same total angular momentum. Off-diagonal interactions between the core-hole spin-orbit components appear to be unimportant, as are contributions from many-body screening effects. No theory is available for the interference involving the hybridized  $d$ -band states. The energies of the edges in electron-energy-loss or x-ray-absorption measurements are shown to be the same within experimental error (about 0.2 eV) as the corresponding values of fully screened core-electron binding energies referenced to the Fermi level. These latter values were determined by Wertheim and coworkers, who fitted the threshold peaks in x-ray-photoemission spectra with a many-body screening theory. It is shown that such agreement between the core-excitation thresholds measured by electron-energy loss or by x-ray absorption and the fully screened binding energies implies that the screening of core holes in Ni and Pt is due almost entirely to the  $d$  conduction electrons.

### I. INTRODUCTION

Coulomb and exchange interactions among the  $d$  electrons and between the  $d$  and core electrons have long been recognized as playing a crucial role in determining the electronic properties of the transition metals.<sup>1</sup> In this paper we explore the consequences of these interactions on the spectral shapes and energies of the core-electron excitation thresholds of the simplest of transition metals, namely Ni and Pt, and of the neighboring noble metals Cu and Au. The main conclusions are: (1) The core-excitation line shapes observed in electron-energy-loss spectroscopy (ELS) and photoabsorption spectroscopy (PAS) for the transition metals are controlled by Fano-type configuration interaction in which the quasisdiscrete *core-d* excitation interferes with a continuum of  $d$ -electron excitations. (2) The final states of core excitations as observed in x-ray-photoelectron spectroscopy (XPS) as well as in ELS and PAS are fully relaxed states in which the core hole is completely screened by  $d$ -valence electrons.

Our choice of the simplest transition metals enabled us to avoid nonessential complications of interpretation and so to establish the conclusions unequivocally. From the point of view of core-

electron spectra, Ni, Pd, and Pt are simple in that they contain a nearly filled  $nd$  conduction band ( $n=3, 4, 5$ ). Thus their ground state consists principally of the  $nd^9 (n+1)s^1$  configuration admixed with some  $nd^{10} (n+1)s^0$ . Excitation of a core electron into the  $d$  conduction band locally results in the excited configuration (core hole)  $nd^{10} (n+1)s^1$ . Such a final state exhibits only the spin-orbit doublet fine structure of the core hole since the  $d$  shell is complete and the exchange interaction between the  $s$  electron and core hole is extremely weak. This will not be the case with the metals in the transition series with atomic numbers below those of Ni, Pd, and Pt, or with the lanthanide and actinide elements, and we shall not consider these more complicated cases in this paper. However, Davis and Feldkamp have recently examined the  $3p$  spectra of Mn atoms in great detail<sup>2</sup> as well as other transition metals in the metallic state.<sup>3</sup>

As early as several decades ago, it was recognized that PAS (Refs. 4-6) and ELS (Refs. 7 and 8) edges in the transition metals were too broad to be interpreted simply as reflecting the conduction-electron density of states. With the recent availability of high-quality synchrotron-radiation-absorption data, a resurgence of interest in these problems has led to new speculations<sup>8</sup> concerning

the shapes of these edges. The basic problem is illustrated in Fig. 1. Here we show a simplified model of a core-excitation edge of a transition metal. The density of states of conduction bands is crudely represented by overlapping rectangular distributions and the Fermi level is indicated near the top of the narrow  $d$  band as is appropriate for Ni, Pd, or Pt. Band-structure calculations<sup>9</sup> indicate that the width at half height of the empty  $d$ -band states is only about 0.3 eV or less in these metals. Since the dipole matrix elements for scattering core electrons of  $f$  or  $p$  symmetry

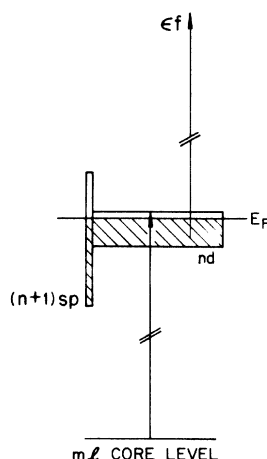


FIG. 1. A schematic diagram of core-excitation edges in transition metals. An electron is excited from an  $ml$  core level into the  $nd$  conduction band. The  $nd$  conduction band consists of two parts: a high-density part as depicted, consisting mainly of unhybridized  $nd$  states, and a low-density hybridized part which makes up roughly half of the  $sp$  band density within a few volts of  $E_F$ . Excitation to the  $(n+1) sp$  states is weak not only because the  $sp$  density of states is small at the edge, but also because the transition matrix element is small. In the cases of Ni and Pt, the width of the empty  $nd$  band state is only about 0.3 eV according to band theory, so that in the absence of configuration interaction (CI) and screening effects, one would expect a sharp spike in the spectral density at the edge. In cases where CI significantly broadens the edge, it is also important to consider the hybridized  $nd$  density in the  $(n+1) sp$  conduction band. For  $l > 0$ , one must also consider the splitting of the core level due to the spin-orbit interaction. In Ni and Pt, which have essentially  $nd^9(n+1)s$  (Ref. 1) ground states, the final states are unsplit by exchange between the core and  $d$  holes since the  $d$  band is locally filled. In the noble metals Cu and Au,  $E_F$  lies above the unhybridized part of the  $nd$  band so that the edge is dominated by excitations to hybridized  $nd$  states in the  $(n+1) sp$  bands. The core excitations are superposed on continua of valence-electron excitations, represented by the upper arrow. If the latter are sufficiently strong, and if the final states are connected by CI, then the core and valence-electron excitations will interfere.

into the empty  $d$ -band states are very much larger than for scattering such electrons into states of  $sp$  symmetry,<sup>10</sup> one may expect to observe a spectral density at the excitation edge of a near delta function which has been broadened to a Lorentzian by the Auger or Coster-Kronig core-hole relaxation. Experimentally this is not always observed, as is shown in Fig. 2 for the case of the  $3p$  and the  $3s$  edges in Ni metal, as measured by scattering 1000 eV electrons from a single crystal (100) surface. While the  $3s$  edge near 110 eV shows a weak peak of the expected shape, the  $3p$  edge exhibits a steplike shape near 65 eV. The  $3p$  line shape was explained by Dietz, McRae, Yafet, and Caldwell<sup>8</sup> as due to an interference effect formally similar to that described by Fano<sup>11</sup> in his treatment of the electron-energy-loss spectrum of He. In the case of the Ni  $3p$  excitation the interference is between the transition matrix elements leading to the excitation of a  $3p$  core electron to the empty part of the  $3d$  conduction band, and those transition matrix elements for the resonant continuum formed by the excitation of  $3d$  electrons into the  $f$  continuum, called  $\epsilon f$ . In the transition metals the interference proceeds via Coulomb and exchange interactions between excited core and excited  $d$ -band electrons. Recently Davis and Feldkamp<sup>2</sup> have demonstrated conclusively that the above described interference process is responsible for the line shapes of the fine structure in Mn  $3p$  vapor spectra, which also shows some similarities to the spectra<sup>12</sup> of Mn metal.

In this paper we report detailed analyses of the line shapes of core excitations measured by ELS

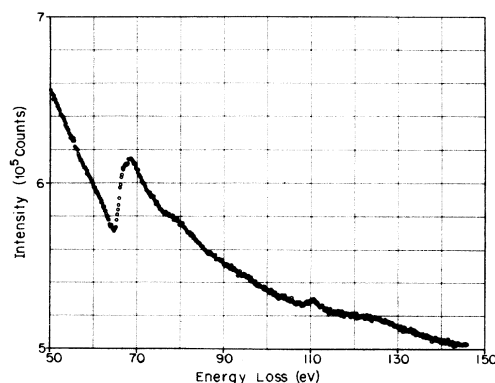


FIG. 2. ELS spectrum obtained by scattering 1000 eV electrons from the (100) surface of nickel. The edge near 65 eV is the  $3p$  spin-orbit doublet while a more symmetrical peak near 110 eV is the  $3s$  edge. The weak features lying some 13 eV above the edges have not been positively identified. The underlying continuum is due to primary and secondary scattering processes involving the conduction (chiefly  $3d$ ) electrons.

for Ni, Pt, Cu, and Au metals. In Pd metal the spectra are too broad to analyze in detail. We also report and analyze PAS results for Pt metal. From these analyses we determine accurate values for the resonant core-excitation energies which are then compared with XPS binding energies for the core level, referenced to the Fermi level. The purpose of this comparison is to determine the extent to which final-state effects arising from Coulomb and exchange interactions are important in and distinguish between the two types of experiments.

To illustrate what we mean by "final-state effects," consider the following single-ground-state-configuration model for excitations in Ni, Pd, and Pt in which an  $np$  electron is excited into the  $nd$  conduction band:

ELS, PAS:

$$np^6nd^9(n+1)s + \hbar\omega - np^5nd^{10}(n+1)s, \quad (1)$$

XPS (unrelaxed):

$$np^6nd^9(n+1)s + \hbar\omega - np^5nd^9(n+1)s + e^-(\text{vac}), \quad (2)$$

XPS (relaxed):

$$np^6nd^9(n+1)s + e^-(\text{cond}) + \hbar\omega - np^5nd^{10}(n+1)s + e^-(\text{vac}). \quad (3)$$

In Eq. (1), an  $np$  electron is scattered into the  $nd$  conduction band, locally completing the  $nd$  shell and fully screening the charge of the  $np$  hole. The spectral density consists of two peaks (these are actually interferences) of unequal intensity separated by the spin-orbit energy of the  $np$  hole. In Eq. (2), an x-ray photon excites an  $np$  core electron into a vacuum state, leaving behind an unrelaxed system consisting of the unscreened  $np$  and  $nd$  holes. The expected spectral density consists of a large number of  $LS$  fine-structure states, split by the combined effects of spin-orbit, crystal-field, and  $np$ - $nd$  hole-exchange coupling. Finally, in Eq. (3) we allow a conduction electron to screen the  $np$  hole by filling the empty  $nd$  orbital in an XPS excitation, thereby creating a fully relaxed final state. This is the most likely possibility for screening the hole since the  $nd$  density is large at  $E_F$  compared to the  $(n+1)sp$  density. While the  $(n+1)s$  electron plays an important role in intra-atomic screening, by reason of its low density of states, it is merely a spectator in the extra-atomic screening of the core hole. The resulting spectral density is again the  $np$  spin-orbit doublet which is the result observed experimentally as shown in Fig. 3 for Ni (Ref. 13) and in Fig. 4 for Pt (Ref. 14). Furthermore, the asymmetric shape of these lines has been noted and explained<sup>14,15</sup> as due to Friedel screening of

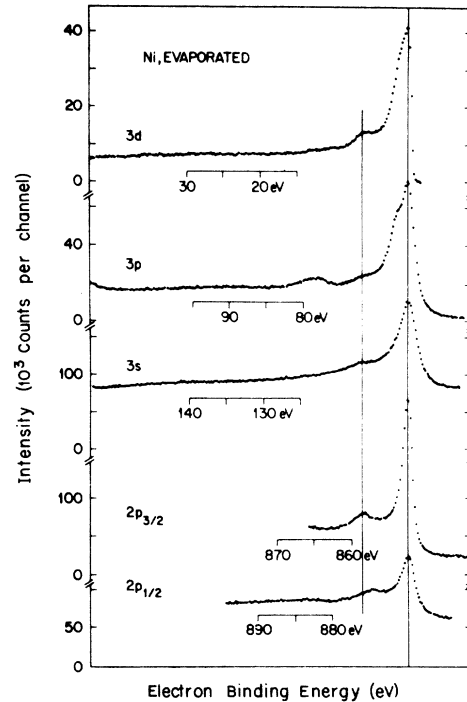


FIG. 3. XPS data for the valence- and core-electron edges of Ni metal measured by Hüfner and Wertheim (Ref. 13). In the  $3p$  spectrum the doublet due to the spin-orbit splitting of the  $3p$  level is unresolved. On all core threshold lines the asymmetry due to many-body screening effects is visible. The vertical lines drawn through the spectra mark the positions of the sideband at 6 eV ascribed (Ref. 13) to the unscreened spectral density, and an unassigned sideband near 12 eV. The latter sideband also appears in the ELS spectra [see Fig. 2(a)].

the core hole.

The local equivalence of the final-state configurations in the two cases [Eqs. (1) and (3)] suggests that the ELS or PAS excitation-energy thresholds should be very close to the XPS binding energy referenced to  $E_F$ . The fact that this is so

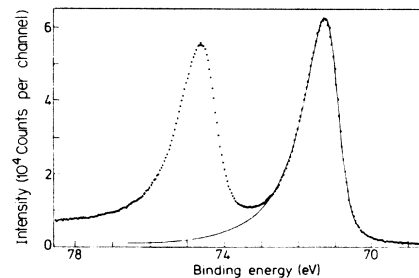


FIG. 4. XPS data for the  $4f$  edges of Pt metal after Wertheim and Walker (Ref. 16). The points are experimental. The smooth curve was obtained by theory including screening processes and  $5d$  band structure (Ref. 16).

can be demonstrated by considering a two-configuration model where the screening electron is taken into account explicitly. We again consider the example of an  $np$  excitation. We let the brackets  $\langle \rangle$  denote the energy of the enclosed configuration; for example, the ground-state energy is  $\langle p^6d^9 \rangle$ . Multiplet averages are assumed where exchange splittings are important. We use  $E_i^i$  to denote the  $i=s$  (screened) or  $i=u$  (unscreened)  $l$ -shell electron binding energy referenced to the Fermi level. The kinetic energy in vacuum of an electron photoexcited from the  $l$  shell is denoted  $e^-(\hbar\omega - E_i^i - \phi)$ , where  $\phi$  is the work function. Then for the resonant ELS or PAS threshold  $\hbar\omega_r$ :

$$\hbar\omega_r + \langle p^6d^9 \rangle = \langle p^5d^{10} \rangle. \quad (4)$$

For the unscreened or Hartree-Fock photoemission thresholds

$$2\langle p^6d^9 \rangle + \hbar\omega = \langle p^5d^9 \rangle + \langle p^6d^9 \rangle + e^-(\hbar\omega - E_p^u - \phi), \quad (5)$$

and for fully screened photoemission thresholds

$$2\langle p^6d^9 \rangle + \hbar\omega = \langle p^5d^{10} \rangle + \langle p^6d^9 \rangle + e^-(\hbar\omega - E_p^s - \phi). \quad (6)$$

The screening energy  $\Delta_s = E_p^u - E_p^s$  is calculated from Eqs. (5) and (6):

$$\Delta_s = E_p^u - E_p^s = \langle p^5d^9 \rangle + \langle p^6d^9 \rangle - \langle p^5d^{10} \rangle - \langle p^6d^9 \rangle. \quad (7)$$

An expression for the screened binding energy of a core electron may be obtained using

$$\langle p^6d^9 \rangle + \hbar\omega = \langle p^6d^8 \rangle + e^-(\hbar\omega - \phi), \quad (8)$$

where  $e^-(\hbar\omega - \phi)$  is the kinetic energy in vacuum of an electron photoexcited from the top edge of the  $d$ -band density of states (the XPS threshold peak). Equations (6), (8), and (4) give

$$E_p^s = \langle p^5d^{10} \rangle - \langle p^6d^9 \rangle = \hbar\omega_r, \quad \text{Q.E.D.} \quad (9)$$

Care must be taken in determining  $E_p^s$  from the XPS threshold peak to correct for the shift due to the finite core-hole lifetime. This can be done by using an appropriate many-body line shape theory.<sup>16</sup>

In writing Eq. (4), we have assumed that the dominant spectral density is that of a Frenkel exciton, in which the excited core electron is bound on the same atom as the core hole. The justification for this assumption is, as we shall see, that the fine structure in the ELS or PAS spectra is that of the spin-orbit doublet of the core hole, suggesting that exchange with holes in the  $d$  band is unimportant. This is consistent with the supposition that the final state is  $d^{10}$ , a closed shell. If the excited electron were to leak out importantly

onto neighboring or more distant atoms so as to form a Wannier exciton, then we would expect to observe an increase in fine structure and a higher mean-threshold energy. The ionization of the exciton state can be represented by a two-atom configuration model:

$$2\langle p^6d^9 \rangle + \hbar\omega_c = \langle p^5d^9 \rangle + \langle p^6d^{10} \rangle. \quad (10)$$

Subtracting Eq. (4) from Eq. (10), we obtain the exciton binding energy  $U_{pd} = \hbar\omega_c - \hbar\omega_r$ :

$$U_{pd} = \langle p^5d^9 \rangle + \langle p^6d^{10} \rangle - \langle p^5d^{10} \rangle - \langle p^6d^9 \rangle. \quad (11)$$

As can be seen in Eq. (11), this is simply the energy required to transfer the excited  $d$  electron from the core-hole site to a distant site. If we let  $U_{da}$  be the increase in energy on transferring a  $d$  electron in the ground state from one site to another,

$$2\langle p^6d^9 \rangle + U_{da} = \langle p^6d^{10} \rangle + \langle p^6d^8 \rangle, \quad (12)$$

then we obtain

$$\Delta_s = U_{pd} - U_{da}. \quad (13)$$

Perhaps the most critical assumption in the above analysis is that the core hole in the XPS final state is screened by an  $nd$  electron. To some extent the core hole will be screened by a  $(n+1)sp$  electron, and to the extent that it is,  $E_p^s$  will deviate from  $\hbar\omega_r$ . As far as our analysis is concerned, it is immaterial whether holes in the  $3d$  band are screened by the  $4sp$  conduction electrons. This is to say that the above relations would be effectively unaltered if  $4sp$  screening electrons were added to each configuration so as to require a total of 16 electrons on each atom. The role of such screening is not established for holes near  $E_F$  and our model is not capable of distinguishing effects due to finite bandwidths.

In any case, one can expect that the difference between  $E_p^s$  and  $\hbar\omega_r$  will be less than the screening energy  $\Delta_s$  as given by Eq. (13). This energy has been estimated from the energy of a weak side-band observed 6 eV on the high-binding-energy side of core threshold XPS lines in Ni metal by Hüfner and Wertheim,<sup>13</sup> as shown in Fig. 3, and attributed by them to the unscreened core-excitation density. This would suggest  $\Delta_s \approx -6$  eV. Alternatively,  $\Delta_s$  can be estimated from Eq. (7) using suitably averaged Hartree-Fock total configuration energies. Watson has kindly calculated the relativistic atomic total configuration energies using wave functions renormalized to the Wigner-Seitz sphere appropriate to Ni metal. We obtain from Eq. (7)

$$\begin{aligned} \Delta_s &= -1516.387 - 1519.305 + 1516.690 + 1519.050 \\ &= 0.048 \text{ hartrees} = 1.3 \text{ eV}. \end{aligned}$$

This figure of 1.3 eV compares poorly with the experimental value of  $-6$  eV. Assuming that the interpretation of the 6-eV sideband in Ni is correct, the fault could lie in our use of the average of configuration energies, lack of self-consistency in the renormalization procedure, neglect of the correlation energy, neglect of  $d$ -band width, and neglect of  $4sp$  screening of  $3d$  holes. Probably all of these factors are significant.

Since we expect that the energy difference between the XPS and ELS core-excitation thresholds will be of order of a few eV at most, it is important that the line shapes of the threshold excitations be understood in detail. With some exceptions,<sup>17-20</sup> previously reported spectra are not adequate for this purpose. Most of them were measured on evaporated films and are somewhat different from one another. These differences have to do with both the shape and structure of the edges, and with the energies of the various features. Some of these differences may arise from oxidation and other imperfections, these problems being particularly acute with data obtained from thin films. The experimental data need to be of good signal quality, measured on clean, well-characterized systems, using an accurately calibrated spectrometer. These conditions are met in obtaining and analyzing our data. As a result we can report that the edge thresholds in PAS and ELS spectra agree in energy with the XPS binding energies referenced to  $E_F$  within the combined experimental uncertainty of 0.1–0.2 eV. This indicates that the interpretation of the XPS threshold energies as corresponding to the fully screened state is well justified. Furthermore, the extremely close agreement suggests that the  $(n+1)sp$  electrons play a negligible role in screening the core hole in the final state. Unfortunately we cannot obtain much useful information on the magnitudes of  $U_{dd}$  and  $U_{pd}$ . If  $U_{pd}$  is not small then the ELS or PAS spectral density will be that of a bound state, rather than being describable as a weighted joint density of states (JDOS) spectrum. In the cases of Ni and Pt, the empty  $d$ -band state density is so narrow that it is difficult to distinguish from such a bound-state density. However, in the case of the  $5p$  edges in Pt, there is strong evidence that the edges are broadened by contributions from  $5d$  states hybridized in the  $6sp$  bands.

## II. EXPERIMENTAL

### A. Procedures for electron scattering experiments

Discs with (100) surfaces were cut from oriented single crystals of Ni, Pd, Pt, Cu, and Au metal. The surfaces were polished with Syton HT30 com-

pound and installed on a Varian precision manipulator in a high-vacuum chamber pumped by conventional ion and titanium sublimation pumps. After bakeout, the pressure was maintained below  $1 \times 10^{-9}$  Torr. The surfaces were monitored by LEED and Auger spectroscopy to verify surface crystallinity and cleanliness. It was generally necessary to clean the surface by argon ion bombardment while heating the sample at  $700^\circ\text{C}$ . For this purpose Ar at a pressure of  $1 \times 10^{-5}$  Torr provided a  $10 \mu\text{A}$  beam of 400-eV ions. The beam energy and temperature were then reduced together after bombarding for about 30 min. This procedure generally left a well-ordered crystalline surface free from carbon and sulfur, the chief contaminants seen in Auger measurements. Samples could be maintained clean for several days without further argon cleaning provided that they were heated to red heat for a few minutes prior to each run. The spectra were recorded with the samples at room temperature.

Both Auger and ELS spectra were recorded using a double-pass cylindrical mirror electrostatic velocity analyzer made by Physical Electronics Inc. A coaxial electron gun was employed for both spectroscopies. Measurements were made in a reflection geometry using primary beam energies of 100–1000 eV in ELS and 3000 eV for Auger. The primary electron beam was incident normal to the crystal surface, while the scattered electrons were collected in a conical sector of  $10^\circ$  at an angle of about  $42^\circ$  to the normal. Beam currents varied correspondingly between 0.1 to  $1.0 \mu\text{A}$  for ELS, and about 2 nA for Auger. The cathode was a thoriated tungsten filament which, with an analyzer pass energy of 15 eV provided a resolution function of 0.50 eV full width at half height. The shape was Gaussian with a partial width of 0.20 eV on the low kinetic energy side, and Maxwellian with a partial width of 0.30 eV on the high kinetic energy side. Both cathode and analyzer retarding potentials were derived from a single high-voltage power supply. An operational supply was introduced in series between the high-voltage supply and retarding grids, and this was controlled by a digital programmer operating through a digital-to-analog converter. The digital programmer produced a digital ramp in response to the channel advance signal of a multichannel analyzer. Discrete electron counts were obtained from a Spiraltron electron multiplier via a low-impedance preamplifier and conventional pulse-counting electronics.

No changes in the core-excitation spectra could be observed by tilting the sample with respect to the analyzer axis, so it was concluded that either or both multiple scattering and large angle col-

lection effectively averaged the scattered electrons with respect to momentum transfer, and to any possible differences between bulk and surface spectral densities. It is generally found that when primary electrons are directed at normal incidence to the surface, the spectral density is almost entirely due to bulk excitation.

Repetitive scans were usually recorded using a dwell time of 1 sec/channel/scan. When the desired signal-to-noise ratio was attained, the data were stored in a computer which eventually produced the figures of this paper. All data points in the figures represent raw data which have been adjusted only to the extent of setting the zero-of-energy loss to the position of the elastic peak.

### B. Procedures for synchrotron radiation absorption experiments

The soft-x-ray-absorption measurements were performed using techniques discussed in detail elsewhere.<sup>5,21</sup> Undispersed synchrotron radiation from Tantalus I (the 240-MeV electron storage ring operated for the NSF by the Synchrotron Radiation Center, University of Wisconsin, Madison) was directed at normal incidence on thin formvar-supported films of Pt ( $\approx 250 \text{ \AA}$ ). The films were prepared in an ion-pumped vacuum system at  $\sim 10^{-7}$  Torr. They were then transferred to the experimental chamber through air. The transmitted radiation was subsequently dispersed by a Hilger-Watts grazing incidence monochromator and was detected by a channeltron with conventional photon-counting electronics. Repetitive scans through the spectral range of interest were made with several different samples using Au, Si, and formvar filters to assess scattered-light and second-order-radiation effects. The determination of the absorption coefficient followed directly from the ratio of the flux transmitted by the sample plus formvar substrate to that transmitted by the substrate alone with corrections for the decaying beam current in the storage ring. The results shown herein represent a single typical scan without signal averaging and covering only a portion of the energy range studied.

## III. RESULTS AND DISCUSSION

### A. Relationship of PAS and ELS line shapes to the dielectric function

In comparing our energy-loss spectra with theory, we assume that the spectra are determined by the bulk spectral density function  $S(\vec{q}, \omega)$ :

$$S(\vec{q}, \omega) \propto -\text{Im}[1/\epsilon(\vec{q}, \omega)], \quad (14)$$

where  $\epsilon \equiv \epsilon_1 + i\epsilon_2$  denotes the bulk dielectric func-

tion. Experiments<sup>20</sup> have shown that the spectral density measured in back reflection on Ni corresponds to a weighted average over  $\vec{q}$ , here denoted  $\bar{S}(\omega)$ . The average is weighted in favor of large  $\vec{q}$  inelastically scattered electrons since they may be back scattered by elastic processes more readily than the small  $\vec{q}$  or forward inelastically scattered electrons. The actual distribution contributing to  $\bar{S}(\omega)$  is unknown but transmission electron scattering experiments<sup>20</sup> indicate that for 1000-eV electrons back reflected from Ni,  $\bar{S}(\omega)$  is proportional to  $S(\bar{q}, \omega)$ , where  $\bar{q} \approx 3A^{-1}$ . The transmission experiments also indicated that the shape of the  $3p$  edge in Ni is independent of  $q$  over the range  $0 < q < 4A^{-1}$ . Thus we can assume that our measurements of  $\bar{S}(\omega)$  approximate  $S(0, \omega)$ . Actually this appears to be true only for that part of the spectral density deriving from the core excitations since it is clear from the  $\vec{q}$ -resolved experiments<sup>20</sup> that the energy dependence of the underlying continua due to excitations of the valence electrons is highly  $\vec{q}$  dependent. Most of these continua are incoherent with respect to excitation of the core electrons and we treat these incoherent continua as a "background" on which we superpose that part of the spectrum relevant to the core excitations.

In interpreting our ELS data, we find that we can (as is often done) interpret our data as roughly proportional to  $\epsilon_2$  using the approximation based on the assumption that  $\epsilon_2 \ll \epsilon_1$ . Thus the energy-loss function  $\text{Im}(-\epsilon^{-1}) = \epsilon_2/(\epsilon_1^2 + \epsilon_2^2)$  reduces to  $\epsilon_2/\epsilon_1^2$ . Since  $\epsilon_1 \approx 1$  for large energy losses,  $\text{Im}(-\epsilon^{-1}) \approx \epsilon_2$ . For example in Pt metal, near the  $4f$  excitation threshold at 70 eV, there is structure due to  $4f \rightarrow 5d$  which spans a difference in absorption coefficient  $\Delta\mu(E) \approx 3 \times 10^5 \text{ cm}^{-1}$ . The underlying continuum or background strength is about  $10^6 \text{ cm}^{-1}$ . Using the formula  $\mu(E) = \omega\epsilon_2/nc$  and assuming that  $n \approx 1$ , we can estimate these contributions to  $\epsilon_2$ : The contribution from the background is  $\epsilon_{B2} \approx 0.2$ , while the contribution from the  $4f$  core excitation to  $\epsilon_2$  is  $\Delta\epsilon_2 \approx 0.06$ .

The decomposition of the energy-loss function into background and "discrete" contributions was described by Davis and Feldkamp<sup>22</sup> as follows. Write for the background dielectric function  $\epsilon_B \equiv \epsilon_{B1} + i\epsilon_{B2}$  and assume that the total dielectric function can be expressed  $\epsilon = \epsilon_B + \Delta\epsilon$ —i.e., the background is incoherent with the discrete part  $\Delta\epsilon$ . With the additional assumption  $\Delta\epsilon \ll \epsilon_B$  one obtains

$$\text{Im}(-\epsilon^{-1}) \approx \text{Im}(-\epsilon_B^{-1}) + A(\Delta\epsilon_2 - r\Delta\epsilon_1), \quad (15)$$

where  $A = \cos 2\theta/|\epsilon_B|^2$ ,  $r = \tan 2\theta$ , and  $\tan \theta = \epsilon_{B2}/\epsilon_{B1}$ . The dependence of  $\epsilon$  on  $\omega$  or energy  $E$  is implicit in these and other similar expressions. Similarly,

for the absorption coefficient  $\mu(E)$ :

$$\begin{aligned}\mu(E) &= \omega \epsilon_2 / nc = (2E/\hbar c) \text{Im}(\epsilon^{1/2}) \\ &= (2E/\hbar c) \text{Im}(\epsilon_B^{1/2} + \Delta\epsilon/2\epsilon_B^{1/2} + \dots) \\ &= \mu_B(E) + (E/\hbar c)A'(\Delta\epsilon_2 - r'\Delta\epsilon_1) + \dots, \quad (16)\end{aligned}$$

where  $A' = \cos(\theta/2)/\epsilon_B^{1/2}$  and  $r' = \tan(\theta/2)$ .

Although the expression for  $\text{Im}(-\epsilon^{-1})$  and  $\mu(E)$  are rather similar, they may produce different line shapes since  $A'$  and  $r'$  differ from  $A$  and  $r$ . As a matter of fact, the experimental ELS and PAS line shapes are very similar for excitations associated with core electrons with binding energies greater than about 60 eV, suggesting that either  $\theta$  is very small or that  $\Delta\epsilon_1$  is small relative to  $\Delta\epsilon_2$ . As we have shown above,  $\epsilon_{B2}/\epsilon_{B1} \approx 0.2$ , so that  $\theta$  is small, of the order of 0.2; in addition it is probably true that  $\Delta\epsilon_1$  is small, since if one assumes a Lorentz oscillator for the transition, it is possible to show that the maximum value of  $\Delta\epsilon_1$  is half the maximum value of  $\Delta\epsilon_2$ , assuming  $\Gamma/\omega_T$  small. Thus both the ELS and PAS spectra can be resolved into a background continuum spectrum which varies slowly with  $E$ , and a superposed discrete spectral feature which is approximately proportional to  $\Delta\epsilon_2$ . This result greatly simplifies the interpretation where applicable: Ni 3*p*, 3*s*; Cu 3*p*; Pt 4*f*; Au 4*f*. It may not be applicable in the case of the Pt 5*p*<sub>3/2</sub> excitation, because of its large oscillator strength and the rapidly varying background. In notations such as 5*p*<sub>3/2</sub> here and elsewhere in this paper, the subscript  $j$  is used where needed to specify a particular spin-orbit component.

#### B. The one-electron transition model

If we neglect all electron-electron and electron-hole interactions, the imaginary part of the dielectric constant  $\epsilon_2$  is given by the matrix-element-weighted joint density of states of a free electron and hole:

$$\begin{aligned}\epsilon_2(\omega) &= \frac{4\pi^2 e^2}{m^2 \omega^2 V} \\ &\times \iint D_e(E) D_h(E') M_{eh}(E, E') \\ &\times \delta(E - E' - \hbar\omega) dE' dE. \quad (17)\end{aligned}$$

We have explicitly summed over the empty densities of states available to the scattered electron and hole  $D_e(E)$  and  $D_h(E')$ . The weighting factor  $M_{eh}(E, E')$  is the square of the scattering matrix element for an excitation of energy  $\hbar\omega$ .

#### The electron density $D_e(E)$

For Ni and Pt the final-state electron density  $D_e(E)$  is essentially a delta function as sketched

in Fig. 1. Band-structure calculations<sup>9</sup> indicate that the full width at half maximum (FWHM) of the empty  $d$ -band states in the two metals is less than 0.3 eV. We can ignore the  $sp$  continuum since calculations by McGuire<sup>10</sup> indicate  $M_{3d,3p} \approx 15M_{4sp}$  in Ni and Cu. For the 4*f* excitations in Pt and Au metal, the dipole matrix elements between the 4*f* and the 6*sp* bands are rigorously forbidden by virtue of the  $\Delta L = \pm 1$  dipole selection rule so that only excitations to the 5*d* and hybridized  $d$  densities are possible. While quadrupole-scattering matrix elements have not been computed for the 3*s* state, the results for our line-shape analysis indicates that  $D_{3d}(E)M_{3d,3s} \gg D_{4sp}(E)M_{4sp,3s}$  in Ni metal near the threshold, and that the delta-function approximation to  $D_e(E)$  is suitable for that case as well. In cases where the finite width of the empty  $d$ -electron states needs to be considered, the density of empty states is represented by Lorentzian distribution of width (FWHM)  $2\Gamma_d$  centered at  $E_F$ . By using a symmetrical distribution, we are apt to underestimate the energy of the edge by  $\sim \Gamma_d$ . The hybridized  $d$  density in the  $sp$  continuum is approximated by a step function at  $E_F$ . Recent tight-binding calculations<sup>23</sup> suggest such an approximation is reasonable. In the case of Ni 3*p* the ratio  $R_h$  of the height of the step to the strength of the essentially unhybridized  $d$  density is taken to be the ratio of the 3*p* threshold step height in Cu to the 3*p* threshold step height in Ni. A similar assumption is made in Pt 4*f* using the observed step height in Au 4*f*.

#### The hole density $D_h(E)$

Because of the small spatial extent of the core-hole wave functions, the core levels are assumed to be nondispersive, and to be split simply by the spin-orbit interaction. Thus  $s$  states are unsplit, while states with  $l > 0$  are doublets characterized by  $j = l \pm \frac{1}{2}$ , the lower multiplicity component occurring at the higher-binding or excitation energy. The lifetime width of the core hole is determined by Auger decay and in most cases is larger than the width of the empty  $d$ -band states. In our analysis this broadening of the  $ml$  core hole is effected by convoluting the spectrum with a Lorentzian whose width (FWHM)  $2\Gamma_m$  is obtained from photoemission data.

#### The scattering matrix element $M_{eh}(E, E')$

Within the scope of this paper, the only important effect  $M_{eh}(E, E')$  has is in determining the relative strengths of the components of the core-hole spin-orbit doublets. The ratios of the strengths of the core-hole doublets are interesting since

the angular momenta of the doublet states are precisely known and may therefore be used to probe the angular momentum of the initial  $d$ -band hole state.<sup>23,24</sup>

To show why this is true, consider the following limiting expressions for the spectral density function, where the  $nd$  spin-orbit splitting  $\lambda_d$  is large or small compared to the  $nd$  bandwidth  $W_d$ :

For  $\lambda_d \gg W_d$

$$S_{jj} \propto \sum_{m, m'} |\langle nd, jm | z | n'l', j'm' \rangle|^2, \quad (18)$$

For  $\lambda_d \ll W_d$

$$S_{jj} \propto \sum_{m, m', j} |\langle nd, jm | z | n'l', j'm' \rangle|^2. \quad (19)$$

Here  $S$  is the line strength of the  $j'$  hole spin-orbit component whose orbital momentum is  $l'$ . We define

$$S_{j'} = \int_0^\infty S_j(\omega) d\omega = \int_0^\infty \omega P_j \cdot \epsilon_2 d\omega / nc; \quad (20)$$

$P_j$  is a projection operator and  $\epsilon_2$  is given by Eq. (17). Provided that  $\lambda_d \ll \omega$ , then the right-hand sides of Eqs. (18) and (19) are independent of  $\omega$ . For Ni  $3p$  excitations,  $S_{5/2, 3/2} / S_{5/2, 1/2} = \infty$  assuming  $\lambda_d \gg \omega_d$ , while  $S_{3/2} / S_{1/2} = 2$  assuming  $\lambda_d \ll \omega_d$ . For the purposes of this paper, we shall be content with treating the line strengths as empirical parameters. However, the line strength parameters obtained in this paper will be compared with those obtained from tight-binding calculations and published elsewhere.<sup>23</sup>

### C. Comparison of the one-electron transition model with experiment

The procedure for fitting the model calculation to the data is as follows. First a background is drawn through the spectrum using a three-parameter fit to describe a parabola:  $B(E) = A + BE + CE^2$ . The resonant energy  $E_0$  (there will be two components for core excitations of  $p$  or  $f$  symmetry) and the lifetime half width of the core hole  $\Gamma_{m_i}$  are taken to be empirical parameters. For measurements in Ni and Pt the half width of the empty  $d$ -band states  $\Gamma_d$  is taken to be an empirical parameter which is simply added to  $\Gamma_{m_i}$  to give the total half width  $\Gamma$ .  $2\Gamma$  is then the total Lorentzian width (FWHM) of the excitation. For Cu and Au edges, the hybridized  $d$  density in the  $sp$  band is represented by a step function which is convoluted by a Lorentzian whose width is determined by the core-hole relaxation rate. For the  $3p$  edge in Ni, and the  $5p$  and  $4f$  edges in Pt, the total  $d$ -hole density is represented by a Lorentzian peak centered at the Fermi energy, added

to a step function at the Fermi energy. The ratio  $R_h$  of the intensity of the step to that of the Lorentzian component is taken to be 1:3 which is the approximate ratio of the strengths of the  $3p$  edge in Cu to that of Ni, and also of the  $5p$  edge in Au to that of Pt. The discrete core-excitation spectrum is added to the fitted continuum or background spectrum, allowing the ratio of the strengths of the two components to be an empirical parameter. Finally, the entire spectrum is convoluted by the experimental resolution function. This latter convolution was not needed for the x-ray data which were recorded with a resolution broadening of only 0.03 eV. The resolution function for the ELS data was obtained from the shape of the elastically scattered electron distribution. This width is only a small fraction of the widths of the observed core excitations with the exception of the Pt and Au  $4f$  edges where the spectral and instrumental widths are about equal.

#### The Ni 3s edge

This case gave the best agreement between experiment and the expected one-electron excitation spectrum. As seen in Fig. 2, the  $3s$  edge near 110 eV takes the form of a sharp, symmetrical peak followed by a broad sideband peaking at some 13 eV higher-energy loss. The significance of the sideband is not certain. It may be due to the excitation of  $3s$  electrons to continuum  $d$ -electron states; but the fact such a sideband is also visible on the photoemission lines in Fig. 3 suggests that it may be a two-electron transition

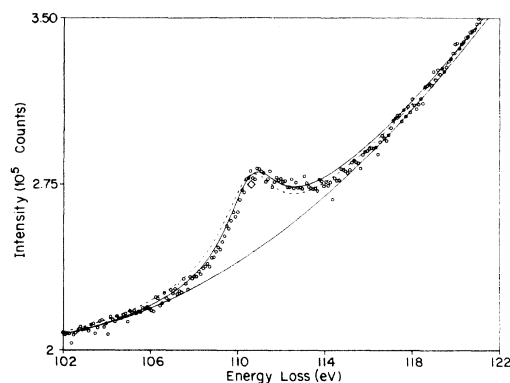


FIG. 5. ELS data for the  $3s$  edge in Ni using 300-eV primary electrons. The points are experimental while the curves are calculated as discussed in the text. The diamond marks the expected binding energy obtained from the line shape analysis. The solid inflectionless curve is the assumed background. The solid and dashed lines fitting the data were obtained by adjusting the spectral parameters to give best fit under the constraint that the background be parabolic. The dashed curve is for the case where  $q = \infty$ , and the solid curve is for  $q = 9$ .

consisting of a core and a valence-electron excitation. Since the 3s excitation in Cu is too weak to be observed, we were not able to determine the ratio  $R_h$  of the hybridized to unhybridized excitation density, so we have simply analyzed the data using the Lorentzian model. This is shown as the dashed line in Fig. 5. The solid line includes interference effects to be discussed later. The parameters  $E_0 = 110.8$ ,  $\Gamma = 1.2$  eV determined from the fit of the model one-electron spectrum to the data are close to the XPS determined parameters<sup>25</sup>:  $E_B = 110.6$ ,  $\Gamma = 1.2$  eV. This correspondence strongly supports the identification of the XPS threshold peak as being the fully screened excitation.

#### The Cu 3p edges

A broad scan of the Cu loss spectrum centering on the 3p threshold is shown in Fig. 6. In this spectrum the scattered electron current decreases initially from the interband loss peaks near 20 eV, and rises again at the 3p edge near 74 eV with a subtle structure which derives from the 3p spin-orbit splitting. In Fig. 7 this edge is shown over a narrow energy scan, together with calculated spectra using step functions to represent the matrix-element-weighted joint density of states. These calculated spectra are convoluted with a Lorentzian function of FWHM 2.0 eV and compare with 1.7 eV from the XPS 3p data.<sup>26</sup> The double-peaked structure in the edge is due to the 3p spin-orbit splitting. The relative weighting  $R_{SO}$  of the two spin-orbit transitions is taken to be 2:1 as determined by the core-hole degeneracy  $2J+1$ . The observed energies of the edges  $E_0(3p_{3/2}) = 75.1$ ,  $E_0(3p_{1/2}) = 77.8$  eV, are close to those given by XPS:  $E_B(3p_{3/2}) = 75.2$ ,  $E_B(3p_{1/2}) = 77.6$  eV. However, the step function does not

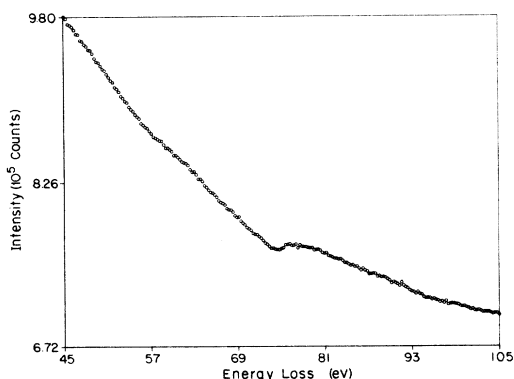


FIG. 6. ELS data for the 3p edge in Cu metal. The diamonds represent the binding energies of the two spin-orbit components as measured by XPS (Ref. 26).

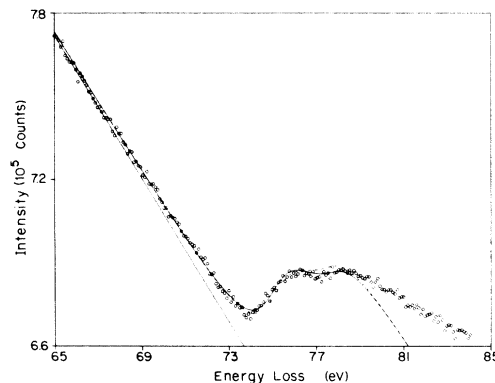


FIG. 7. ELS data for Cu 3p edges similar to Fig. 6 but on an expanded scale. The spin-orbit splitting is apparent. The lines were calculated assuming that the edges were not interferences, and that the spectral density could be represented by step functions. The dashed curve gives a fit using a value for the spin-orbit splitting of 2.4 eV as measured by XPS (Ref. 26) while the solid line represents the case where the splitting is 2.7 eV.

well describe the shape of the continuum. The continuum is made up of states of  $s$ ,  $p$ , and  $d$  symmetry, with the states at threshold being made up principally of  $p$  and  $d$  character.<sup>27</sup> At higher energies the observed increase in the scattering relative to that expected for a step function may possibly be due to an increasing contribution of continuum  $d$  final states, although this is not expected if one considers hybridization only with the  $3d$  orbitals. Alternatively it might be symptomatic of an interference between the semicontinuum of  $3p$  core-electron excitations and the continuum of  $3d$  electron excitations. Such an interference due to configuration interaction cannot be represented by a Fano theory<sup>11</sup> as has been done for the  $3p$  excitation in Ni metal,<sup>8</sup> but requires a new theory in which a semicontinuum interferes with a continuum. In Fig. 7, the background was determined by the assumption that the core excitation was incoherent with the underlying continuum. If interference effects are important in Cu as they are in Ni  $3p$ , then the  $3p$  edge in Cu could be anticipated by destructive interference at energies below the edge and followed by constructive interference above the edge. The background curve in such a case would lie *above* the data for energies below the edge, and below the data for energies above the edge. Possibly the observation of resonant photoemission from Cu  $3p$  could illuminate this question. In Cu as in Ni  $3s$ , the energies of the ELS and XPS thresholds are identical, indicating that the XPS peak energy is the fully screened binding energy. In this case, however, the electron screening takes place in a

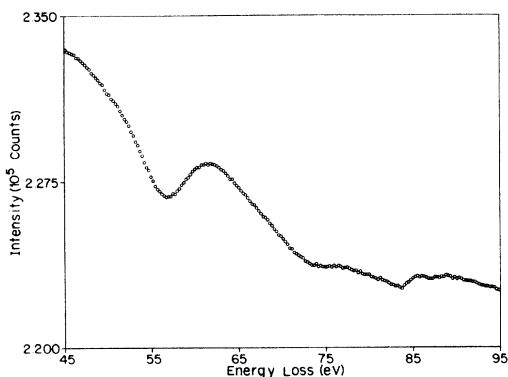


FIG. 8. ELS for Au showing the  $5p$  and  $4f$  excitation edges. The diamonds give the XPS binding energies for the  $5p$  levels (Ref. 26). Notice that the binding energies for the  $5p$  levels occur at the minima of the spectral density, suggesting that the  $5p$  edges are interferences.

broad conduction band in which Coulomb interactions are expected to be much weaker. Because of the crudity of the edge measurements in the present case the observed coincidence of ELS and XPS should not be considered to be a critical test of core-hole screening in Cu.

#### The Au $5p$ and $4f$ edges

From a band-structure point of view, the situation in Au is almost identical to that of Cu. As shown in Fig. 8, four distinct edges can be identified:  $5p_{3/2}$  with a threshold near 57 eV,  $5p_{1/2}$  near 74 eV (the positions marked with diamonds are the relaxed XPS binding energies<sup>26</sup>), and sharper thresholds near 84 and 87 eV for the  $4f_{7/2}$  and  $4f_{5/2}$  edges.<sup>28</sup> While the  $5p_{3/2}$  edge is particularly well resolved, it is apparent that the shape of the edge cannot agree with a simple one-electron model since the XPS binding energy occurs near the *minimum* of the spectral density contributing to the edge, rather than halfway up as would be the case for a Lorentzian-broadened step function. Furthermore, the background is concave downward, i.e.,  $d^2S/dE^2 < 0$ , near the onset of the edge—a signal that an interference effect may be present. While the  $5p_{1/2}$  edge is much weaker, it appears to be otherwise similar to the  $5p_{3/2}$  edge.

In the case of the  $4f$  edges, the spectrum appears to be in much better agreement with one-electron theory than the  $5p$  edges are and this is as it should be for two reasons: Firstly, the  $4f$  excitations occur at higher energy than the  $5p$  excitations so that their background is smoother,  $\epsilon_{B2}$  is smaller,  $\Delta\epsilon_2$  is smaller, and  $\epsilon_1$  is close to unity; secondly, the  $4f$  holes are very long lived  $2\Gamma_{4f} \approx 0.3$  eV due to the weakness of the radial overlap with higher-lying (lower binding

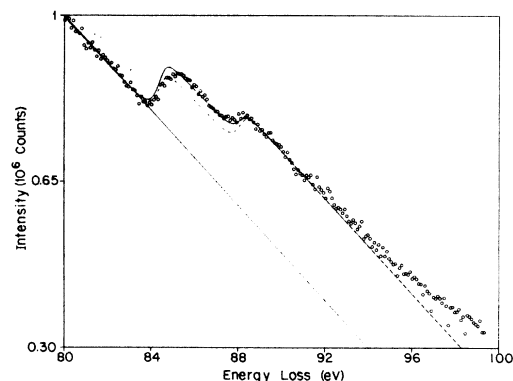


FIG. 9. ELS data for the Au  $4f$  edges shown on an expanded scale, together with spectra calculated assuming no interferences and step functions for the spectral densities. The lifetime and instrumental broadening of the experimental edges are not well described by the calculations. It is not clear whether this is due to an experimental artifact or to lack of consideration of broadening due to many-body screening or configuration-interaction interference effects. However, good agreement is reached between the observed positions of the edges and the calculated edges indicated by the diamonds which are based on values measured by XPS.

energy) electrons. The  $5p$  holes on the other hand overlap well with the  $5d$  electrons and consequently are short lived ( $2\Gamma_{5p} \approx 3.5$  eV) with respect to OVV Coster-Kronig relaxation. This relaxation is a manifestation of configuration interaction which has been shown to be responsible for the strong interferences in the  $p$  edges of the transition metals.<sup>8</sup> We suggest that interferences are important in the  $p$  edges of the noble metals as well.

As shown in Fig. 9, the calculated spectrum which is based on the XPS binding energies is in good agreement with the observed  $4f$  edges, and in this case the edges also seem to be well characterized as step functions. Values of  $E_0$  obtained from fitting the model spectrum are  $E_0(4f_{7/2}) = 84.5$  and  $E_0(4f_{5/2}) = 88.0$  eV. We also remark that in this spectrum the final electron density can only be that of the continuum  $d$  states which are made up of hybridized  $5d$  and higher-lying  $d$  orbitals. Excitation of  $f$  electrons to orbitals of  $s$  and  $p$  character are forbidden by the  $\Delta l = \pm 1$  selection rule for dipole transitions, and  $g$  orbitals will contribute negligibly near the Fermi edge because of centrifugal-barrier effects. In Fig. 9 the ratio  $R_{SO}$  of the  $4f_{7/2}$  edge strength to that of the  $4f_{5/2}$  edge is taken as a parameter for best fit to the data. We obtain a value of 2.5 for this ratio which may be compared to the corresponding ratio of the degeneracies of the  $4f$  core holes which is 4:3. The observed deviation

from the 4:3 ratio is due to a preponderance of empty  $5d_{5/2}$  states which are hybridized into the  $6sp$  conduction bands, and is in excellent agreement with calculations of this effect.<sup>23</sup>

#### Failure of the one-electron excitation model

The one-electron excitation model fails completely to describe the Ni  $3p$  and the Pt  $5p$  and  $4f$  excitations. Figure 10 displays attempts to fit the  $3p$  edge in Ni as we have done in the previous cases. Here instead of using the step function we assume that the dominant feature is due to the narrow, relatively unhybridized spike of empty  $3d$ -band states just above the Fermi level, as shown in Fig. 1, except that we give the peak in the  $3d$  empty DOS a Lorentzian width of 0.3 eV. The hybridized  $d$ -band states are represented as before by a step function, and the spectrum is convoluted with a Lorentzian whose width is determined by the core-hole lifetime. Finally, the entire spectrum is superposed on a linear background and convoluted with the resolution function. This is then plotted in Fig. 10 for three different ratios of the hybridized- $3d$  to unhybridized- $3d$  density at the Fermi edge, and compared to the experiment. The

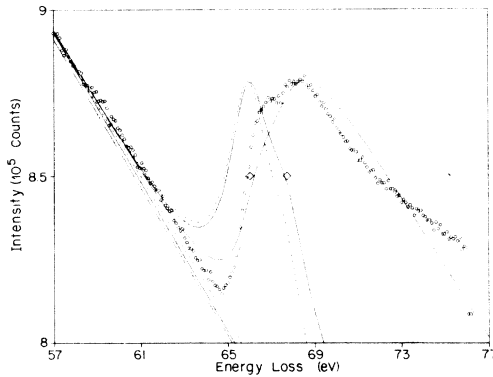


FIG. 10. The ELS data of Fig. 2 for the  $3p$  edges in Ni presented on an expanded energy scale, together with edge shapes calculated in the one-electron approximation using different relative strengths of hybridized  $3d$  to unhybridized  $3d$  spectral densities. The dashed, solid, and dot-dashed curves, respectively, represent the cases where the ratios  $R_h$  of hybridized to unhybridized  $3d$  spectral density are 0, 0.33, and  $\infty$ . The strength of the unhybridized distribution is taken as the height of a Lorentzian with width  $\Gamma=0.3$  eV centered at  $E_F$ . The strength of the hybridized part is taken to be the height of the step function. The diamonds represent the XPS binding energies (Ref. 29). The assumed backgrounds are linearly extrapolated from the data below the edges: In the absence of interference they cannot “anticipate” the onset of the edge. While the best fit is given by the step distributions, the edge in that case is too broad, and the step distribution is physically unreasonable.

background is assumed incoherent with the core excitation in this model and is therefore extrapolated linearly through the  $3p$  resonance region. The resonance energies are taken equal to the XPS binding energies, and the linewidths are as determined by XPS:  $2\Gamma_{3p}=1.7$  eV.<sup>26</sup> The ratio  $R_{SO}$  of the strengths of the spin-orbit components is taken to be 2:1. The calculated lines are arbitrarily normalized to the peak of the data. The dashed line corresponds to the assumption that the transition matrix element to the hybridized  $3d$  states is zero. Although this distribution is obviously too narrow, the spin-orbit components are not resolved as well as the data and appear in the wrong intensity ratio. The full line shows results of adding a contribution from hybridized- $3d$  states so that the ratio of hybridized- $3d$  to unhybridized- $3d$  strength is  $R_h=0.33$ . The dot-dashed curve gives the case where the continuum  $d$  states have all of the strength, and while the energy and intensities are in better agreement in this case, the shape of the edge is wrong and the spin-orbit structure is unresolved. Since the ratio of continuum to discrete strengths is at most 0.33 judging from the relative strengths of  $3p$  excitations in Cu and Ni, the last case is clearly unreasonable, and we look to electron-electron interaction effects for an explanation.

#### D. Interference line shapes

The slightly concave downward piece of the spectrum in Ni  $3p$  just above 60 eV suggested that an interference effect was important here and it was so proposed in an earlier publication.<sup>8</sup> The success of this approach is realized if one introduces a single constant parameter  $q$  into the line shape calculation. This parameter controls the asymmetry of the line shapes according to the Fano theory<sup>11</sup> which describes in a very general way the interference between a discrete transition and a resonant continuum:

$$\frac{S(\omega)}{S_M(\omega)} = \frac{(q + \epsilon)^2}{1 + \epsilon^2}, \quad (21)$$

where  $S(\omega)$  is the total spectral strength,  $S_M(\omega)$  is the strength of the coherent continuum,  $q$  is the asymmetry parameter, and  $\epsilon$  is a reduced energy:  $\epsilon = (E - E_0)/\Gamma$ , where  $\Gamma$  is the linewidth parameter ( $2\Gamma = \text{FWHM}$ ),  $E = \hbar\omega$ , and  $E_0$  is the discrete transition energy.

In order to calculate a spectrum we make the following assumptions.

(1) The parameters  $S_M(\omega)$ ,  $E_0$ ,  $q$ , and  $\Gamma$  are all assumed to be energy independent. Since in most cases the total assumed background intensity varies only 10–15% over the energy interval fitted, this would seem to be an upper limit to the

energy dependence of the parameters. Provided that the energy dependence of  $S_M(\omega)$  can be neglected,  $E_0$ ,  $q$ , and  $\Gamma$  would be energy dependent only if there were off-diagonal elements in the configuration-interaction matrix which connect the two spin-orbit components of the  $3p$  hole state.<sup>22</sup> Such off-diagonal elements are absent in spherical symmetry (i.e., the atomic case) where  $J$  is a good quantum number, but may be present in cubic or lower symmetry or if the final-state  $d$ -band configuration is not a closed shell. In that case, exchange terms may multiply the number of final states characterized by a particular  $J$  quantum number. We have carried out calculations of line shapes in Ni and Pt, where we have included such off-diagonal elements as parameters, but find that their main effect is to alter the relative intensities of the spin-orbit components. Since the relative intensities of the Ni  $3p$  and of the Pt  $4f$  components seem to be adequately described by band theory,<sup>23</sup> we are inclined to assume that such off-diagonal elements are small. This assumption is much better in Pt, where  $\Gamma$  is small relative to  $\Delta_{SO}$  the spin-orbit splitting:  $2\Gamma/\Delta_{SO} \approx 0.1$ , for Pt compared to  $2\Gamma/\Delta_{SO} \approx 1$  for Ni.

(2) We assume that the background is a sum of an energy-dependent part together with an energy-independent part. Only the energy-independent continuum is coherent with the core excitation. In effect we assume that the incoherent continuum is simply added to the total coherent spectral strength  $S(\omega)$  obtained from Eq. (21). This is, of course, implicit in the one-electron calculations in Fig. 10. The parameter specifying the relative fraction of coherent and incoherent continuum is not arbitrary since the coherent part contains a zero which establishes the scale.

(3) We fix the ratio of hybridized  $3d$  to unhybridized  $3d$  strength at  $R_h = 0.33$ . This is somewhat arbitrary since it is difficult to accurately calibrate the relative strength of the edges in Cu and Ni, and also because the matrix elements are expected to differ somewhat between Cu and Ni. Nevertheless, we expect the 0.33 ratio to be reasonably accurate, and in any case the fit to the observed line shapes is not very sensitive to the amount, if any, of hybridized  $d$  contribution. Lacking a suitable theory for determining the effect of configuration interaction on the shape of the core-to-hybridized  $d$  excitation, we have approximated the shape of that part as we did in Cu by a step function.

#### Configuration-interaction effects in the Ni $3p$ edge

To obtain the best fit of the calculated line shapes to the data, we have allowed the binding

energies to depart slightly from the XPS values. In Fig. 11 we use  $E_0(3p_{3/2}) = 66.0$  and  $E_0(3p_{1/2}) = 67.9$  eV. The XPS values are<sup>29</sup>  $E_B(3p_{3/2}) = 65.9$  and  $E_B(3p_{1/2}) = 67.7$ . In Fig. 11 the calculated spectra given by the solid and dashed curves, respectively, correspond to different ratios  $R_{SO}$  of  $3p_{3/2}$  to  $3p_{1/2}$  final-state spectral densities 2.4 and 2.0. The value  $R_{SO} = 2.4$  gives an extremely close fit to the data for the energy region extending to a few eV above the edge. The fitted shapes should actually fall below the data in that region because of the broad sideband excitation which peaks some 13 eV above the edge. The value for the asymmetry parameter which was found to give best fit to the spectrum was  $q = 1.30$ , while the value for  $2\Gamma_{3p} = 1.8$  eV was identical to the XPS value. Thus both excitations studied in Ni, the  $3p$  and the  $3s$ , have ELS (or PAS) resonances in excellent agreement with their XPS binding energies. *Such agreement implies that the core-electron threshold peaks in photoemission are fully screened excitations in which the screening charges are mainly  $d$  electrons*

In Fig. 12 we show the sensitivity of the fit to

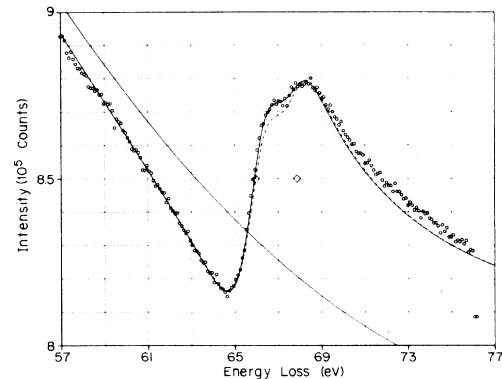


FIG. 11. The effect of including configuration-interaction interference effects in the theory given in Fig. 10. The line shapes are determined by the same parameters used in Fig. 10, together with a single additional parameter (the asymmetry parameter  $q$ ). In addition, the fitted curves are constrained by requiring the background to be a parabola. The fit above 70 eV is poor because of the contribution of additional scattering channels near 78 eV. The calculated spectra given by the solid and dashed curves, respectively, correspond to different ratios  $R_{SO}$  of  $3p_{3/2}$  to  $3p_{1/2}$  final-state spectral densities: 2.4:1 and 2:1. The fact that the observed value is larger than the statistical value (2:1) can be understood by considering the distribution of total angular momentum states in the  $3d$  band (Ref. 23). The binding energies represented by diamonds in the figure were obtained from the line shape analysis. They lie within 0.2 eV of the measured XPS values. The value assumed for  $\Gamma_d$  was 0.3 eV. The ratio  $R_h$  of the (Lorentzian-broadened) hybridized to unhybridized  $3d$  densities was 0.33.

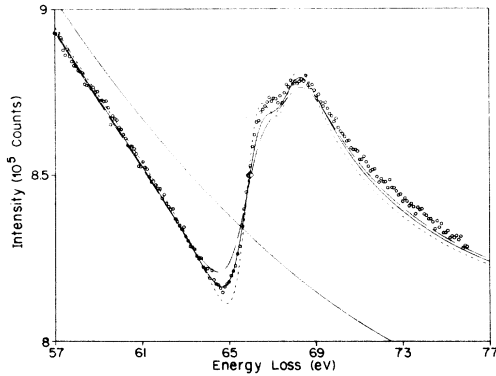


FIG. 12. The effect of the width of the ground-state  $3d$ -hole density on the Ni  $3p$  line shape. The solid line corresponds to the case of the dashed line in Fig. 11 with  $2\Gamma_d = 0.6$  eV. The dashed curve is computed with  $2\Gamma_d = 0$ , and the dot-dashed curve is computed with  $2\Gamma_d = 1.2$  eV.

the width  $2\Gamma_d$  of the Lorentzian density of states assumed to represent the empty unhybridized states in the  $3d$  band. The solid line is the same as the dashed line given in Fig. 11 with  $2\Gamma_d = 0.6$  eV. The dashed line in Fig. 12 corresponds to  $\Gamma_d = 0$ , while the dot-dashed line corresponds to  $2\Gamma_d = 1.2$  eV. Thus the additional width over that due to the hole lifetime is somewhat larger than the width given by the  $3d$  band-structure calculations (about 0.3 eV FWHM). It seems likely that the additional width is due to inadequacies in our treatment of the hybridized  $d$  states, but it could also be due to an experimental artifact or to neglect of other processes such as many-body effects.

#### Possible many-body screening effects in Ni $3p$ edges

We have explored the possible role of the many-body screening effects on the line shapes  $A(\alpha, \omega)$  by applying the convolution line shape theory of Mahan<sup>30</sup> to the spectral density  $H_0(\omega)$  including the configuration-interaction effect. For  $\alpha < 0$ ,

$$A(\alpha, \omega) = \int_{-\infty}^{\infty} d\omega' H_0(\omega - \omega') B(\alpha, \omega'), \quad (22)$$

where

$$B(\alpha, \omega) = \frac{\theta(\omega)}{\Gamma(-\alpha)\omega} \left(\frac{\xi_0}{\omega}\right)^\alpha e^{-\omega/\kappa_0}.$$

For  $\alpha > 0$ ,

$$A(\alpha, \omega) = \left(1 + \xi_0 \frac{\partial}{\partial \omega}\right) A(\alpha - 1, \omega). \quad (23)$$

The definitions of the parameters are as given by Mahan.<sup>30</sup>

While the assumed form of the broadening function  $B(\alpha, \omega)$  is admittedly crude when applied

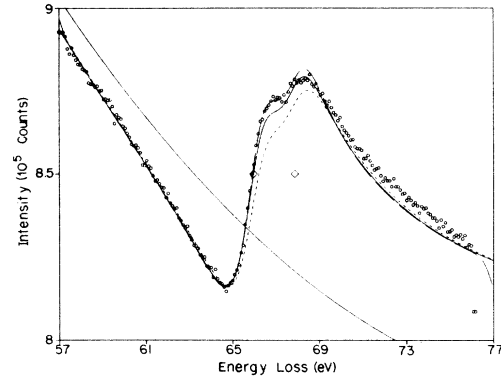


FIG. 13. The effect of Friedel screening on the line shapes. The solid curve corresponds to the dashed curve of Fig. 11, i.e., with  $\alpha$  in Eq. (22) set equal to zero. The dot-dashed curve corresponds to  $\alpha = +0.1$ , and the dashed curve corresponds to  $\alpha = -0.03$ . While there is a tradeoff between the effects of changing  $\alpha$  on the one hand, and changing the spin-orbit intensity ratio  $R_{so}$  and  $\Gamma_d$  on the other, it appears that  $\alpha$  must be small and lie in the range of the values employed in this figure.

to a narrow band of states, it should give a qualitative indication of the importance of screening effects on the ELS or PAS spectral density in the vicinity of the edge. Figure 13 shows the result of assigning different values to the parameter  $\alpha$  while keeping all other parameters constant and letting  $\xi_0 = 2.0$  eV. The solid line gives the fit indicated by the dashed line in Fig. 11, with  $\alpha = 0$ . The dot-dashed line shows the spectrum with  $\alpha = -0.03$ , and the dashed line is that for  $\alpha = +0.1$ . These results show that screening plays only a minor role in determining the ELS and PAS edges in the transition metals.

The minor role of many-body screening in ELS is in contrast to substantial effects for the same transitions in XPS. For example, the Ni  $3p$  XPS line exhibits a very substantial many-body asymmetry. The difference is probably due to partial cancellation between the contributions to the asymmetry index  $\alpha$  from screening of the core hole and of the excited  $d$  electron, respectively. For ELS or PAS edges the cancellation is expressed<sup>31</sup>

$$\alpha = \frac{2\delta_2}{\pi} - g, \quad (24)$$

where  $g$  denotes the XPS singularity index and has the following expression in terms of partial-wave atomic-scattering phase shifts  $\delta_l$ :

$$g = 2 \sum_l (2l + 1) \left(\frac{\delta_l}{\pi}\right)^2.$$

If we use our conclusion from the coincidence of the XPS and ELS edge energies that mainly  $d$

electrons participate in screening the core hole, and further restrict the values of the phase shifts by the Friedel sum rule  $2\sum_i (2l+1)(\delta_i/\pi) = 1$ , we have  $\delta_2 = \pi/10$  so that  $g = 0.1$  and  $\alpha = 0.1$ . This result should correspond to the case of Pt since we have allowed screening by both spins. This result is not appropriate to Ni where the  $d$ -band electrons at  $E_F$  are spin polarized. If one removes the factors of two from Eq. (24) and the Friedel sum rule, then one obtains  $g = 0.2$  (as observed)<sup>29</sup> and  $\alpha = 0.0$ . Obviously these estimates are very crude, as other phase shifts will contribute to some extent and the free-electron form of the Friedel sum rule is inappropriate for a real band structure. However, they do tend to support our conclusion that *screening effects will be minimal in the PAS and ELS edges in the transition metals.*

*The significance of  $q$ ,  $\Gamma$ , and  $E_0$  in Ni 3p edges*

In the Fano theory<sup>11</sup>  $\Gamma_i$  is interpreted as the linewidth of the discrete excited state  $i$ , which in our case is the excited core-hole- $d$ -conduction-electron pair. In the transition metals,

$$\Gamma_i = \pi \sum_j V_{ij}^2, \quad (25)$$

where  $V_{ij}$  represents a configuration-interaction matrix element connecting the core-hole-conduction-electron pair state  $|i\rangle$  with a continuum  $|j\rangle$ . The continuum may be represented as a hole in either another core level or in the valence band, with the excited electron in a conduction state. The matrix elements  $V_{ij}$  are formed from weighted combinations of two-electron integrals: the direct (or Coulomb)  $J(a, b) \equiv \langle ab' | a'b \rangle$  and the exchange  $K(a, b) \equiv \langle ab' | ba' \rangle$ . These are given here in the notation of Condon and Shortley.<sup>32</sup> Both  $J$  and  $K$  contribute to the same final-state configuration  $\langle ab' |$  but via different processes: If we suppose that the crystal is excited by scattering an electron from an occupied orbital  $a$  to an unoccupied orbital  $a'$  via the transition matrix element  $P_i \equiv \langle a' | T | a \rangle$ , then  $J(a, b)$  represents the relaxation process whereby the electron in  $a'$  relaxes directly back into  $a$ , while at the same time scattering an electron from an initially occupied state  $b$  into an excited state  $b'$ . Likewise,  $K(a, b)$  corresponds to the process where an electron in  $b$  relaxes into  $a$ , while the initially excited electron in  $a'$  is scattered into  $b'$ . *Resonance* occurs if  $P_i$  corresponds to the core-electron excitation while  $M_j \equiv \langle b' | T | b \rangle$  corresponds to the excitation of an overlapping continuum of excitations  $b'$ . *Interference* between  $P_i$  and  $M_j$  will then take place if either  $J(a, b)$  or  $K(a, b)$  are nonzero. In the Fano theory for the interference of a single

discrete transition  $P_i$  with a nondegenerate continuum  $M_j$ , the asymmetry of the spectral line is determined by the asymmetry parameter  $q_i$ , where

$$q_i = P_i / \left( \pi \sum_j M_j V_{ij} \right). \quad (26)$$

Equation (26) recognizes that there may be continua  $M_j$  which are incoherent with the discrete transition  $P_i$  because  $V_{ij}$  are zero by symmetry; similarly there are configuration-interaction processes  $V_{ij}$  which cause state  $|i\rangle$  to relax into states  $|j\rangle$  for which there are no corresponding resonant continua  $M_j$ . The former of these processes results in the incoherent background in PAS or in ELS; the latter processes manifest themselves as that part of the Auger electron emission which is incoherent with the one-electron excitation spectrum. All processes  $V_{ij}$  contribute to the linewidth through Eq. (25) and to the asymmetry through Eq. (26).

In the case of the 3p excitation in Ni metal, the ground state is essentially  ${}^2D$  with a roughly statistical mix of  ${}^2D_{5/2}$  and  ${}^2D_{3/2}$ . The 3p core-electron states are  ${}^2P_{3/2}$  and  ${}^2P_{1/2}$ . These discrete transitions (discrete because the *empty* part of the essentially unhybridized part of the 3d band is narrow in energy, not because the  $d$  electrons are localized in space, as implied in a recent publication<sup>33</sup>) interfere with the resonant continua of excitations of the 3d electrons  $\epsilon p$  and  $\epsilon f$ . The following matrix elements have been estimated<sup>8</sup> using McGuire's atomic Herman-Skillman matrix elements for the radial parts, together with the appropriate angular factors:  $P(3p^5 3d^{10} 4s ({}^2P_J))$ ,  $M(3p^6 3d^8 4s \epsilon p ({}^2P_J))$ , and  $M(3p^6 3d^8 4s \epsilon f ({}^2P_J))$ ;  $J(\epsilon f) = \langle 3p \epsilon f; 3d', 3d \rangle$  and  $K(\epsilon f) = \langle 3p \epsilon f; 3d, 3d' \rangle$  [and similarly for  $J(\epsilon p)$  and  $K(\epsilon p)$ ]. The  $M(\epsilon p)$  matrix elements were found to be small compared to  $M(\epsilon f)$  so that the contribution of the  $M(\epsilon p)$  continuum was neglected. It turns out that while  $K$  is smaller than  $J$ , the number of  $K$  terms that enter is much larger so that exchange processes outweigh the direct processes in contributing to the resonance effects. The calculated values<sup>8</sup> are  $q = 1.8$  and  $2\Gamma = 4$  eV. McGuire<sup>34</sup> has recently suggested that the discrepancy between the calculated and measured values for  $\Gamma$  may be due to the use of Herman-Skillman functions rather than Hartree-Fock ones.

$E_0$  represents the energy of the discrete core excitation in the absence of the configuration interaction. Fano<sup>11</sup> has shown that the observed resonance energy is given by  $E_0 + F(E)$  where  $F(E)$  is a self-energy correction due to the interaction.  $F(E) = P \int dE' |V_E|^2 / (E - E')$ , where  $P$  indicates that the principal part is to be taken.

If  $V$  is independent of  $E$ , then  $F(E)$  vanishes. Judging from the excellence of the fit of the simple Fano line-shape theory to the experimental data for Ni and for Pt (below), we conclude that the assumption of energy-independent matrix elements is justified and that  $F(E)$  is either small or does not vary significantly within a linewidth or two of  $E_0$ . Naturally, if the resonance is well characterized by an energy-independent parameter  $F$ , that parameter will also contribute to the XPS binding energy measured at the threshold peak provided that the XPS screened final-state configuration is the same as that of the ELS or PAS final state.

#### Configuration-interaction effects in the Ni 3s edge

As shown by the Fano formula, Eq. (21), in general interference effects will be important for values of the asymmetry parameter  $q$  of about one or less. Estimates of  $q$  based on Eq. (26) indicate  $q \leq 1$  for almost all core excitations below 100 eV. Exceptionally large  $q$  values are found for some of the lighter atoms, where there are only  $s$  and  $p$  electrons. In those cases the valence-continuum matrix element  $M$  falls off relatively rapidly with increasing energy.

Using the above rule of thumb, it is rather puzzling why the Ni 3s excitation shows little asymmetry compared to the 3p one. For example, the solid line in Fig. 5 shows a fit for  $q = 9.0$  which is about the smallest value of  $q$  that can give a reasonable fit to the spectrum. To account for this value of  $q$  by Eq. (26), either the configuration-interaction matrix element  $V$  or the continuum transition matrix element  $M$  must be assigned an exceptionally small value. The transition responsible for the 3s edge is essentially  ${}^2D - {}^2S$ , so that the continuum involved has  $S$  symmetry. The possibility that  $V$  is small would be realized if the radial parts of the contributing matrix elements such as  $\langle 3s\epsilon s; 3d3d \rangle$  and  $\langle 3s\epsilon s; 3p3d \rangle$  were small compared, for instance, to the corresponding matrix elements controlling the configuration interaction in the 3p case. The other possibility, namely, that  $M$  is small, would be realized if the coherent continuum were relatively weak near the 3s edge compared to the 3p edge. This is plausible because the 3s edge is 40 eV higher than the 3p edge and the  $S$ -symmetry continuum  $\epsilon s$  can be expected to fall off much more rapidly with excitation energy than  $\epsilon f$  due to centrifugal-barrier effects in the latter case.

#### Configuration-interaction effects on the 5p edges of Pt

We now attempt to apply the same fitting procedure used in the case of the 3p edge in Ni to the

case of the 5p edges in Pt. At first sight the 5p edges might seem a more favorable case for analysis than the 3p edges of Ni. The  $5p_{3/2}$  and  $5p_{1/2}$  excitations are spin orbit split by 15 eV, which is large compared with their widths due to Auger recombination (about 3.6 eV). Thus the two edges are completely resolved. On the other hand, the lifetime width is sufficiently broad that the spectral density of the unoccupied unhybridized 5d density when convoluted over this width is little stronger than the hybridized 5d density.

In Fig. 14 an attempt is made to fit the 5p edges using a Lorentzian distribution width  $2\Gamma_d = 0.3$  eV for the unhybridized 5d-hole density and a step function for the hybridized 5d density with a ratio of  $R_h = 0.33$  as determined by comparing the respective edge strengths in Au and Pt. The solid curve gives a fit by adjusting the relative strengths of the  $5p_{3/2}$  and  $5p_{1/2}$  spectra such that the ratio of strengths is  $R_{SO} = 6.7$ . The dashed curve gives the statistical case  $R_{SO} = 2:1$ . Since the 5d spin-orbit splitting relative to the 5d band width is larger in Pt than in Ni, one expects that the 5d-hole angular momentum in the ground state will be mainly  $J = \frac{5}{2}$ , and this would lead to a larger intensity ratio as observed.<sup>23,24</sup> The total linewidth  $2\Gamma = 4.0$  eV chosen for this fit is slightly larger than the sum of the XPS value of 3.6 eV<sup>26</sup> for the width of the 5p-hole state and  $2\Gamma_d$ . However, this value for  $\Gamma$  is clearly too small to fit the observed spectrum. Since the unhybridized 5d density is narrow, as may be judged from the

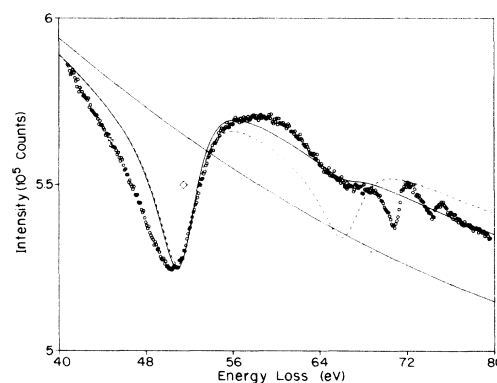


FIG. 14. ELS for Pt showing the 5p excitation edge. The diamonds give the XPS binding energies for the 5p levels (Ref. 26):  $E_B(5p_{3/2}) = 51.9$ ,  $E_B(5p_{1/2}) = 66.9$  eV (the second diamond is almost obscured by data points). The dashed and solid curves are attempted fits using intensity ratios for  $5p_{3/2}$  to  $5p_{1/2}$  spin-orbit components  $R_{SO} = 2$  (statistical value) and  $R_{SO} = 6.7$ , respectively. The inflectionless solid line is the background. The linewidth parameter  $2\Gamma = 4.0$  eV used for this fit is clearly too narrow (see text).

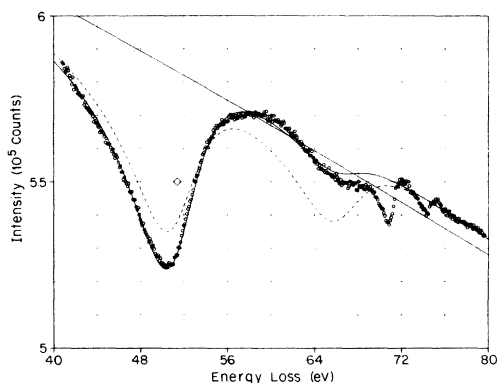


FIG. 15. ELS data for Pt identical to that in Fig. 14, together with fits obtained with linewidth  $2\Gamma = 7.9$  eV. The dashed and solid curves are fits using  $R_{50} = 2$  and  $R_{50} = 6.7$ , respectively. The diamonds give transition energies adjusted to fit the data. Note that the  $5p$  transition energies  $E_0$  are near the minima, just as in the case of Au (Fig. 8).

sharpness of the  $4f$  edges near 72 eV, one must assume that the inadequacy of our fitting procedure in the  $5p$  case must arise from the fact that we have not included the hybridized  $5d$  density in the configuration interaction process. Since the width of the unhybridized  $d$  density is of the same order of magnitude as the lifetime width of the core hole, we can, in this case, crudely approximate the line shape by lumping both hybridized and unhybridized  $5d$  densities together into a Lorentzian distribution and leave the width of this distribution as a parameter to be adjusted. In Fig. 15, we show the best fit attained by this procedure using a total width for the unoccupied  $5d$  density of  $2\Gamma_d = 4.3$  eV, which is an order of magnitude larger than the width of the unhybridized  $5d$ -hole density. The quality of this fit suggests that our procedure is reasonable, and that the hybridized  $5d$  density is involved in the interference via the configuration interaction process in a way very similar to that of the unhybridized part. The fitted resonance energies  $E_0(5p_{3/2}) = 51.3$ ,  $E_0(5p_{1/2}) = 66.3$  eV were close to the XPS binding energies.<sup>26</sup> We would expect that owing to our fitting procedure  $E_0$  should be shifted about  $\Gamma_d \sim 2$  eV higher in energy due to the strong contribution of the hybridized  $d$  states. The fact that this is not observed may be due to inadequacies in our model for the interference with the hybridized  $5d$  states. Alternatively it may indicate a degree of excitonic localization in the final state which distorts and shifts the spectral density due to the  $d$  electrons towards the Fermi energy.

The background curve used in this analysis is the smooth solid line (Fig. 15) which decreases

monotonically with energy from the interband peaks near 30 eV. The solid fitted curve was computed so as to give best fit to the data, while ignoring the  $f$  excitations near 72 eV. While these  $4f$  excitations are quite narrow and possess little oscillator strength, they nevertheless contribute to the spectral strength at 80 eV, mainly because of contributions from continuum  $d$  states. The solid line can be taken as an approximate background curve for the analysis of the  $4f$  excitations under the assumption that the  $4f$  excitations do not interfere materially with the  $5p$  density, or that if they do we may still treat the relevant matrix elements as being energy independent.

#### Configuration-interaction effects in the Pt $4f$ edges

The Pt  $4f$  edges present the most favorable opportunity for studying the effects due to configuration-interaction on the edge shapes since the  $4f$  core-hole lifetime is very long, resulting in sharp, well-resolved lines. The linewidth due to Auger decay of the core hole is just  $2\Gamma_{4f} = 0.25$  eV, while the  $5d$ -hole width in the ground state is about  $2\Gamma_d = 0.30$  eV making a total width of about  $2\Gamma = 0.55$  eV. This is a small fraction of the spin-orbit splitting of 3.4 eV.<sup>16</sup> The fitting procedure is carried out as for the Ni  $3p$  edge, in that we use a step function for the hybridized  $5d$  density and allow configuration-interaction only with the unhybridized  $5d$  density. The resulting line shapes are plotted for the ELS data in Fig. 16, with the solid line as before corresponding to the adjusted fit of the ratio of the intensities of the two spin-

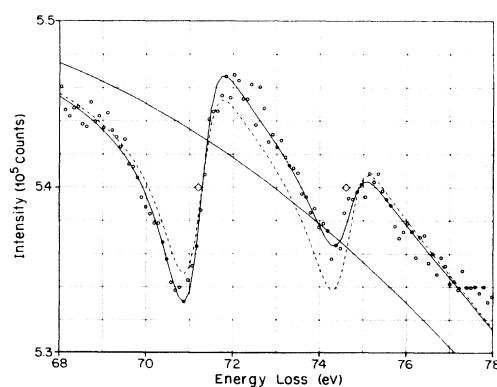


FIG. 16. The ELS data of Fig. 14 showing the  $4f$  edges on an expanded energy scale. The dashed and solid curves are fits using intensity ratios for  $4f_{7/2}$  to  $4f_{5/2}$  spin-orbit components  $R_{50} = 4:3$  (statistical value) and  $R_{50} = 2.5$ , respectively. The observed deviation from the statistical ratio has been ascribed to  $5d$  band-structure effects (Ref. 23). The diamonds give transition energies adjusted to fit the data. They are within 0.2 eV of the measured XPS core-level binding energies (Ref. 16).

orbit components. The dashed line uses the statistical value  $R_{SO} = 4:3$ . The parameters used in the fit are  $q = 0.55$ ; ratio of line strengths  $R_{SO} = S(4f_{7/2})/S(4f_{5/2}) = 2.5$ ;  $2\Gamma_d = 0.3$ ;  $2\Gamma_{4f} = 0.25$ ;  $E_0(4f_{7/2}) = 71.20$ ;  $E_0(4f_{5/2}) = 74.60$  eV; and  $R_h = 0.17$ , where the  $R_h$  is the ratio of hybridized (step function)  $5d$  density to unhybridized  $5d$  density.

The background curve is not well represented by a parabola in this case because of the proximity of the broad, weak  $5p_{1/2}$  excitation near 66 eV, which causes the background continuum to be concave down. At sufficiently high energies above  $5p_{1/2}$  the continuum would again assume a concave up shape and this effect causes the background to deviate from the data near 78 eV. Most of the parameters are extremely close to values fixed by other means. XPS measurements give  $2\Gamma_{4f} = 0.25$  eV;  $E_B(4f_{7/2}) = 71.2$ ;  $E_B(4f_{5/2}) = 74.6$ . Synchrotron radiation measurement of the relative strengths of the  $4f$  edges in Au (Ref. 35) and in Pt give  $R_h = 0.17$ . Band theory<sup>23</sup> gives the values  $R_{SO} = S(4f_{7/2})/S(4f_{5/2}) = 2.5$ ,  $2\Gamma_d = 0.30$ , and  $R_h = 0.25$ .

We show in Fig. 17 analogous data obtained from synchrotron-radiation-absorption measurements. These data were recorded under much higher resolution (about 30 meV) than the ELS measurements although the data have been collected into 0.1-eV channels. A similar fitting procedure was used as for the ELS data except that the calculated spectrum was not convoluted by a resolution function. The fit was obtained with  $q = 0.80$ ,  $R_{SO} = 2.3$ , and other parameter values the same as for the ELS data of Fig. 16. The main difference lies in the value obtained for  $q$ . It is possible that the difference in the value of  $q$  obtained in the two experiments can be attributed to the fact that the dielectric function is sampled somewhat differently in the two experiments as indicated by Eqs. (15) and (16). Davis and Feldkamp<sup>22</sup> have shown that  $q$  tends to be somewhat lower in an ELS experiment than in a photoabsorption experiment, although the Fano line shape function is still valid. Another possibility is that the quality of the sample may affect  $q$ . The differences are only slightly larger than the uncertainty in the fitting procedure. In the case of the photoabsorption data, background appears to be more strongly perturbed by the  $5p_{1/2}$  line than in the ELS spectra, although this is difficult to see from the segment of data shown in Fig. 17. The values for  $E_0$  obtained from the photoabsorption measurements fall within the estimated error of the values obtained by ELS. Since the ELS measurements were considered more accurate with respect to energy calibration, the PAS data were calibrated by the ELS energies.

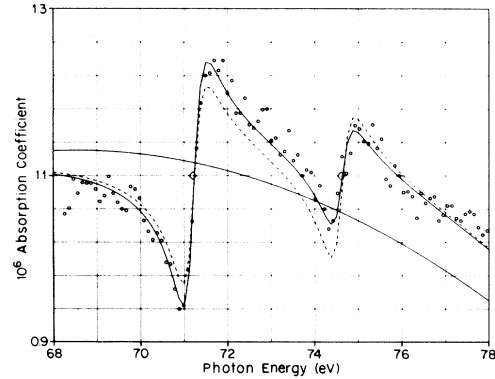


FIG. 17. Synchrotron-radiation, absorption data for the  $4f$  excitation edges in Pt. These data are very similar to those of Fig. 16. The dashed and solid curves are fits using ratios of  $4f_{7/2}$  to  $4f_{5/2}$  spectral densities  $R_{SO} = 4:3$  (statistical value) and  $R_{SO} = 2.3$ , respectively.

The width of the empty unhybridized  $d$ -band states  $2\Gamma_d = 0.3$  eV is just that suggested by band theory. This measurement is particularly precise since the width is actually larger than that due to the  $4f$ -hole relaxation, both widths being appreciably larger than the experimental resolution. This measurement is consistent with the larger  $\Gamma_d$  widths observed in the  $5p$  excitation in Pt as well as in the  $3p$  edges in Ni. In those cases the hybridized  $d$ -hole density is relatively more important because of the larger linewidths due to Auger relaxation.

#### IV. CONCLUSIONS

The core-excitation line shapes observed in ELS and PAS for the transition metals are controlled by Fano-type configuration interaction in which the quasiscrete *core-d* excitation interferes with a continuum of  $d$ -electron excitations. The excitation energies  $E_0$  may be determined accurately ( $\pm 0.2$  eV) by fitting the observed line-shapes using the Fano line shape formula. The experimental values of  $E_0$  are shown in Table I together with the corresponding XPS binding energies  $E_B$  and related quantities.

The difference between  $E_0$  and  $E_B$  values indicates the extent of screening of core excitations. If the XPS threshold peaks were due to an unscreened spectral density, the difference would be  $U_{cd} - U_{dd}$ , where  $U_{cd}$  is the core-exciton binding energy and  $U_{dd}$  is the  $d$ -electron Coulomb repulsion energy.  $U_{cd} - U_{dd}$  is of the order of a few eV. However,  $E_0$  and  $E_B$  are the same within experimental error (Table I) indicating that the core excitations are completely screened by  $d$  electrons. The shapes of ELS or PAS edges for

TABLE I. Parameters obtained by fitting core-electron excitation edges with model line shapes.

Metal	Core level <sup>a</sup>	$E_B$ (XPS)	$E_0$	$2\Gamma_{\text{core}}$ (XPS)	$2\Gamma_d$	$q$	$R_{\text{SO}}$
Ni	$3p_{3/2}$	65.9	66.0	1.7	0.6	1.3	2.4
	$3p_{1/2}$	67.7	67.9	1.7	0.6	1.3	...
	$3s$	110.6	110.8	1.2	0.3	>9	...
Cu	$3p_{3/2}$	75.2	75.1	1.7	0.3	...	2
	$3p_{1/2}$	77.6	77.8	1.7	0.3	...	...
Pt	$5p_{3/2}$	51.9	51.5	3.6	3	0.32	6.7
	$5p_{1/2}$	66.9	66.5	3.6	3	0.32	...
	$4f_{7/2}$	71.2	71.2	0.25	0.4	0.55	2.5
	$4f_{7/2}$ (PAS) <sup>b</sup>	71.2	71.2	0.25	0.3	0.80	2.3
	$4f_{5/2}$	74.6	74.6	0.25	0.4	0.55	...
Au	$4f_{5/2}$ (PAS)	74.6	74.6	0.25	0.3	0.80	...
	$5p_{3/2}$	57.2	na <sup>c</sup>	3.5	na	...	...
	$5p_{1/2}$	74.3	na	3.5	... <sup>d</sup>	...	...
	$4f_{7/2}$	84.4	84.5	0.24	0.4	...	2.3
	$4f_{5/2}$	88.1	88.0	0.24	0.4	...	...

<sup>a</sup>The notation is  $ml_j$  where  $m$  is the principal quantum number of the core hole.

<sup>b</sup>PAS = photoabsorption spectroscopy.

<sup>c</sup>na = not analyzed.

<sup>d</sup>... = not applicable.

the Ni 3s and 3p, and Pt 4f excitations are particularly well described by the configuration interaction between  $L_{l\pm 1/2}$  discrete states and  $L_{l\pm 1/2}$  continuum states where  $L=l$ . The discrete states consist locally of an  $l$ -angular-momentum core hole and a filled  $d$ -valence shell. The resonant continua consist of an additional hole in the  $d$  band with an electron excited above the vacuum level. The configuration interaction appears to be effectively diagonal with respect to a basis characterized by the total angular momentum  $J$ . This suggests that the relative intensities of spin-orbit multiplet components are mainly determined by  $d$ -electron band-structure effects. Such intensity ratios  $R_{\text{SO}}$  as listed in Table I are in close agreement with recent tight-binding calculations for Pt and Au (Ref. 22).

There is little evidence for many-body screening effects in ELS and PAS for transition metals, even in cases where such effects are known to be important for XPS.

In cases like Cu and Au where the Fermi level lies above a filled  $d$  band, excitations of core and valence electrons are also observed to interfere. In these cases the principal contribution to the

spectral density is thought to be valence-band  $d$  states which are hybridized with the conduction bands of  $sp$  symmetry. These excitations, which may be characterized as interferences between continua (the valence-electron excitations) and semicontinua (the core-electron excitations), cannot be described well by the Fano model, and these edges as yet have no adequate theoretical description.

#### ACKNOWLEDGMENTS

We are grateful to R. L. Campbell for assistance with the measurements, to W. F. Flood who prepared the samples, to R. E. Watson for certain total-energy calculations, to Y. Yafet for a critical reading of the manuscript and numerous suggestions, to G. K. Wertheim and S. Hüfner for unpublished data, and to M. Campagna, L. C. Davis, J. D. Dow, L. A. Feldkamp, C. Herring, S. Hüfner, G. D. Mahan, A. E. Meixner, P. M. Platzman, E. A. Stern, R. E. Watson, and G. K. Wertheim for useful discussions. The Synchrotron Radiation Center is operated under NSF Grant DMR 7721888; the support of the Synchrotron Radiation Center staff is gratefully acknowledged.

<sup>1</sup>C. Herring, in *Magnetism*, edited by G. T. Rado and H. Suhl (Academic, New York, 1966), Vol. IV.

<sup>2</sup>L. C. Davis and L. A. Feldkamp, *Phys. Rev. A* **17**, 2012 (1978).

<sup>3</sup>L. C. Davis and L. A. Feldkamp, *Solid State Commun.*

**19**, 413 (1976).

<sup>4</sup>D. H. Tomboulion and P. L. Hartman, *Phys. Rev.* **102**, 1423 (1956). A more recent survey of the  $3p$  edges of the first transition series has been made by B. Sonntag, R. Haensel, and C. Kunz, *Solid State Commun.* **7**,

- 597 (1969). See also R. Bruhn, B. Sonntag, and H. W. Wolff, DESY Report No. SR-73/14 (unpublished) for studies of atomic and metallic Fe, Co, Ni, and Cu.
- <sup>5</sup>The  $4p$  edges have been reported in J. H. Weaver and C. G. Olson, *Phys. Rev. B* **14**, 3251 (1976).
- <sup>6</sup>The  $5p$  edges have been discussed in R. Haensel, K. Radler, B. Sonntag, and C. Kunz, *Solid State Commun.* **7**, 1495 (1969).
- <sup>7</sup>J. L. Robins and J. B. Swan, *Proc. Phys. Soc. London* **76**, 857 (1960).
- <sup>8</sup>R. E. Dietz, E. G. McRae, Y. Yafet, and C. W. Caldwell, *Phys. Rev. Lett.* **33**, 1372 (1974).
- <sup>9</sup>See, for example, L. Hodges, H. Ehrenreich, and N. D. Lang, *Phys. Rev.* **152**, 505 (1966).
- <sup>10</sup>E. J. McGuire, Sandia Laboratories Report No. SC-RR-710835, 1972 (unpublished).
- <sup>11</sup>U. Fano, *Phys. Rev.* **124**, 1866 (1961).
- <sup>12</sup>J. P. Connerade, M. W. D. Mansfield, and M. A. P. Martin, *Proc. R. Soc. London* **A350**, 405 (1976). R. Bruhn, B. Sonntag, and H. W. Wolff, DESY Report No. SR-78/16 (unpublished).
- <sup>13</sup>S. Hüfner and G. K. Wertheim, *Phys. Lett.* **51A**, 299 (1975).
- <sup>14</sup>S. Hüfner and G. K. Wertheim, *Phys. Rev. B* **11**, 678 (1975).
- <sup>15</sup>S. Hüfner and G. K. Wertheim, *Phys. Lett.* **51A**, 301 (1975).
- <sup>16</sup>G. K. Wertheim and L. R. Walker, *J. Phys. F* **6**, 2297 (1976).
- <sup>17</sup>We find that some of the spectra reported in the literature for Ni appear to be very similar to those we report here. In particular we cite the photoabsorption data of Brown *et al.* (Ref. 18). They assigned two peaks in the  $3p$  edge near 65 eV to the two spin-orbit components  $3p_{3/2}$  and  $3p_{1/2}$ . We concur with that assignment. High-energy electron-transmission measurements (Refs. 19, 20) also reveal similar structure to that which we report here, with particularly close agreement obtained in the case of the data of Meixner *et al.* (Ref. 20) for Ni  $3p$  and  $3s$  edges.
- <sup>18</sup>F. C. Brown, C. Gähwiller, and A. B. Kunz, *Solid State Commun.* **9**, 487 (1971).
- <sup>19</sup>L. C. Davis and L. A. Feldkamp (unpublished).
- <sup>20</sup>A. E. Meixner, R. E. Dietz, G. F. Brown, and P. M. Platzman, *Solid State Commun.* **27**, 1255 (1978).
- <sup>21</sup>C. Gähwiller, F. C. Brown, and H. Fujita, *Rev. Sci. Instrum.* **41**, 1275 (1970); C. Gähwiller and F. C. Brown, *Phys. Rev. B* **2**, 1918 (1970).
- <sup>22</sup>L. C. Davis and L. A. Feldkamp, *Phys. Rev. B* **15**, 2961 (1977).
- <sup>23</sup>R. E. Dietz, L. F. Mattheiss, and J. H. Weaver, in *Transition Metals, International Physics Conference Series*, edited by M. J. G. Lee, J. M. Perz, and E. Fawcett (Institute of Physics, Bristol and London, 1978), Vol. 39, p. 145; and L. F. Mattheiss and R. E. Dietz (unpublished).
- <sup>24</sup>M. Brown, R. E. Peierls, and E. A. Stern, *Phys. Rev. B* **15**, 738 (1977).
- <sup>25</sup>G. K. Wertheim (unpublished). See also Ref. 13.
- <sup>26</sup>G. K. Wertheim (unpublished).
- <sup>27</sup>See, for example, Refs. 9 and 23.
- <sup>28</sup>Y. Yafet and G. K. Wertheim, *J. Phys. F* **7**, 357 (1977).
- <sup>29</sup>See Ref. 26. An earlier determination by S. Hüfner and G. K. Wertheim, *Phys. Lett.* **51A**, 301 (1975) did not properly take into consideration the band-structure effects discussed in Ref. 13.
- <sup>30</sup>G. D. Mahan, *Phys. Rev. B* **14**, 3702 (1976).
- <sup>31</sup>P. Nozières and C. T. De Dominicis, *Phys. Rev.* **178**, 1097 (1969).
- <sup>32</sup>E. U. Condon and G. Shortley, *The Theory of Atomic Spectra* (Cambridge University, London, 1935).
- <sup>33</sup>M. B. Stearns and S. Shinozaki, *Physica* **86-88B**, 1195 (1977).
- <sup>34</sup>E. J. McGuire, *Phys. Rev. A* **16**, 2365 (1977).
- <sup>35</sup>H.-J. Hagemann, DESY Report No. F41-74/4 (unpublished).